Dalton Transactions

Accepted Manuscript

This article can be cited before page numbers have been issued, to do this please use: M. Caterino, A. A. Petruk, A. Vergara, G. Ferraro, D. Marasco, F. Doctorovich, D. Estrin and A. Merlino, *Dalton Trans.*, 2016, DOI: 10.1039/C6DT01685E.

ROYAL SOCIETY OF CHEMISTRY

www.rsc.org/dalton

Dalton Transactions

Dynamic Article Links►
View Article Online
DOI: 10.1039/C6DT01685E

Cite this: DOI: 10.1039/c0xx00000x

www.rsc.org/xxxxxx

ARTICLE TYPE

Mapping the protein-binding sites for iridium(III)-based CO-releasing molecules

Marco Caterino[‡], *Ariel A. Petruk*[†], *Alessandro Vergara*[‡,#], *Giarita Ferraro*[‡], *Daniela Marasco*[¥,#], *Fabio Doctorovich*[†], *Dario A. Estrin*[†], *Antonello Merlino*[‡,#,*]

Received (in XXX, XXX) Xth XXXXXXXXX 20XX, Accepted Xth XXXXXXXXX 20XX
DOI: 10.1039/b00000

A combination of mass spectrometry, Raman microspectroscopy, circular dichroism and X-ray crystallography has been used to obtain detailed information on the reaction of the iridium-based CO-releasing molecule (Ir-CORM) Cs_2IrCl_5CO with the model protein bovine pancreatic ribonuclease. The results show that Ir-compound fragments bind to N-terminal amine and close to histidine and methionine side chains, retaining the CO ligand for a long time. Data provide helpful information to identify protein targets for Ir-CORMs and for studying the mechanism that allows them to exhibit their interesting biological properties.

The properties of some metal-containing compounds in the treatment of selected human diseases are known since thousands of years. However, after the important success of cisplatin and its derivatives in the treatment of tumors, the interest of the scientific community towards the synthesis and characterization of potential drugs based on metal compounds has been sensibly grown. In recent years numerous complexes of Ru, Ti, Fe, Au, Ag, V, Bi, Sb, Os and Ir have been tested as pharmacological agents. The mechanism of action of these compounds are not entirely deciphered, but it is clear that DNA is not always the primary target, as for Pt based drugs[1-3].

The study of the interaction of metal based drugs with proteins is thus of crucial importance to unveil the mechanism of actions of these important pharmacological agents and several reviews have been published in this field.[4-6]

Among the metal-based drugs, CO-releasing molecules (CORMs)[7-10] based on complexes of Mn, Fe, Co, Ru and Ir [9,11-14] are drawing increasing attention among medicinal (inorganic) chemists because of their promising bactericidal,[11] anti-inflammatory,[15,16] anti-apoptotic,[17] anti-microbial[18] and anti-proliferative properties.[19]

To understand the biological properties of these CORMs in detail, it is important to characterize their interactions with the possible biological targets, to define the binding sites of the metal, and to determine which among the original ligands are still present upon the formation of the adduct. The binding of CORMs to proteins can play an important role in their activation, transport, and excretion in vivo.[20] A few structural studies of protein-CORM adducts have been performed, but the knowledge of how CORMs recognize proteins and the mechanism which allows CORMs to release CO in the presence of a protein is still rather limited. Crystallographic studies on the first protein-CORM adduct, carried out using hen egg white lysozyme (HEWL) as model protein, have demonstrated that the Ru complex CORM-3 can bind to surface histidine and aspartic residues.[21] Subsequently, it has been shown that ruthenium-based CORMs can bind HEWL at diverse sites, *i.e.* close to His15, Asp18, Asp101 and Asp119.[22-24] Recently, we have performed a structural characterization of the adducts that are formed when HEWL reacts with the Ir-based CORM Cs_2IrCl_5CO.[14,25] It is found that adducts can be formed via either covalent or non-covalent interactions. Six different binding sites have been identified (His15 (site 1); Ser24, Asn27, and Val120 (site 2); Asn65 and Pro79 (site 3); Asp18 (site 4); Asn59, Trp62, Trp63, and Ala107 (site 5); and Asn46 and Thr47 (site 6)), although His15 seems the primary anchoring site for the Ir derivatives. Loss of CO in the crystal state has been also observed both via X-ray crystallography and Raman microspectroscopy.[25]

In our continuous efforts to unveil the molecular bases of metallodrug-protein interactions, here we have investigated the reactivity of Cs_2IrCl_5CO with the model protein bovine pancreatic ribonuclease (RNase A) using mass spectrometry (MS), X-ray crystallography and Raman microspectroscopy. The stability of the adduct formed upon reaction of the protein with the potential metallodrug has been also evaluated by circular dichroism.

Experimental Section

Crystallization and data collection

Crystals of the adduct formed in the reaction between RNase A (Sigma Chemical Co, XII A) and $IrCl_5CO^{2-}$ have been obtained by the soaking procedure. In particular, crystals of RNase A have grown in two weeks by the hanging-drop vapour-diffusion method using a reservoir solution containing 22% PEG4K and 10 mM sodium citrate at pH 5.1. They have been soaked with a saturated solution of Cs_2IrCl_5CO. After four days (crystal 1) and two months (crystal 2) of soaking, these crystals were fished with a nylon loop, flash-cooled without cryoprotectants at 100 K using nitrogen gas produced by an Oxford Cryosystem and dehydrated

View Article Online
DOI: 10.1039/C6DT01685E

at air[26], as done in other works.[27-29]

Data have been collected at 1.85 and 2.29 Å resolution for crystal 1 and 2, respectively, at the CNR Institute of Biostructure and Bioimages, Naples, Italy, using a Saturn944 CCD detector equipped with CuKα X-ray radiation from a Rigaku Micromax 007 HF generator and processed using HKL2000.[30] Details of data collection statistics are reported in Table 1.

Structure solution and refinement

The structures of the two RNase A-$IrCl_5CO^{2-}$ adducts have been solved with Phaser, using the A chain of the PDB file 1JVT as starting model.[31] As expected,[31-32] these crystals contain two molecules in the asymmetric unit (molecule A and molecule B). The refinements have been carried out with CCP4 Refmac5 [33] using NCS restraints; model building, map inspections and model adjustments have been manually performed with Coot.[34] The structures refine up to R-factor/R-free values of 0.172/0.226 and 0.224/0.293 for crystal 1 and crystal 2, respectively. Table 1 reports the refinement statistics. Figures were created using UCSF Chimera Package.[35] The refined structural models and structure factors have been deposited in the Protein Data Bank as entries 5JMG and 5JML for crystal 1 and crystal 2, respectively.

Table 1. Data collection and refinement statistics

Data collection	***Crystal 1***	***Crystal 2***
PDB code	5JMG	5JML
Space group	C2	C2
Unit cell parameter		
a (Å)	99.9	99.6
b (Å)	32.6	32.4
c (Å)	72.3	72.6
α(°)	90.0	90.0
β (°)	90.3	90.0
γ(°)	90.0	90.0
Observed reflections	55190	24425
Unique reflections	19871	10756
Resolution (Å)	72.27-1.85 (1.88-1.85)	72.59-2.29 (2.34-2.29)
Completeness (%)	97.8 (93.5)	96.5 (97.8)
Rmerge (%)	6.3 (40.6)	13.9 (55.7)
I/σ(I)	10.9 (2.3)	10.7 (2.0)
Multiplicity	2.8 (1.7)	2.3 (2.3)
Refinement		
Resolution (Å)	72.27-1.85	72.59-2.29
Number of reflections in working set	18853	9837
Number of reflections in test set	1017	490
R factor (%)	17.2	22.4
Rfree (%)	22.6	29.3
Rall (%)	17.5	22.7
Number of non-hydrogen atoms	2238	2027
Mean B-value (Å)	26.4	35.5
Ramachandran plot statistics		
Most favoured/Additional allowed (%)	95.1/4.5	95.1/4.5
Generously allowed/ Disallowed (number of residues)	0/1	0/1
R.m.s.d. bonds (Å)	0.016	0.012
R.m.s.d. angles (°)	2.4	2.5

Values in parenthesis refer to last resolution shell

Raman microspectroscopy

Raman microscopy spectra on RNase A crystals and on crystals of the RNase A-$IrCl_5CO^{2-}$ adduct have been collected at the Department of Chemical Sciences of University of Naples Federico II, using an apparatus and a procedure described elsewhere[36]. Raman spectra of Cs_2IrCl_5CO powder have been collected as a reference as well. The excitation line was 514 nm, with a power at the sample of 3 mW. The spectra resolution was 7 cm^{-1}.

Mass spectrometry

MS analysis has been performed on an LCQ DECA XP Ion Trap mass spectrometer (ThermoElectron, Milan, Italy) equipped with an OPTON ESI source (operating at 4.2-kV needle voltage and 320°C) Mass spectra have been recorded continuously between the mass range 400–2000 Da in positive mode. Multicharge spectra were deconvoluted using the BioMass program implemented in the Bioworks 3.1 package provided by the manufacturer.

Circular dichroism

CD spectra of RNase A and of the adduct formed between the protein and $IrCl_5CO^{2-}$ after 24 h of incubation in 1:1 and 1:10 protein to metal ratio have been recorded at 10 °C using a Jasco J-710 spectropolarimeter equipped with a Peltier thermostated cell holder (Model PTC-348WI) (Jasco, Easton, MD). The mean residue molar ellipticity, [θ] in deg cm^2 $dmol^{-1}$, has been calculated from the equation:

$$[\theta] = [\theta]_{obs} \times MRW/(10lc)$$

Where $[\theta]_{obs}$ is the ellipticity measured in degrees, MRW the mean residue molecular weight, c is the protein concentration in g mL^{-1} and l is the optical path length of the cell in cm.

Far-UV measurements (190–250 nm) have been carried out using a 0.1 cm path length cell and protein concentration 0.1 mg mL^{-1} in a 10 mM Tris-HCl buffer, pH 7.4. Before measurements, the instrument has been calibrated with an aqueous solution of d-10-(+)-camphorsulfonic acid at 290 nm. Thermal unfolding curves for the protein and the adduct have been recorded in the temperature mode at 222 nm in the same experimental conditions (protein concentration 0.1 mg mL^{-1} in a 10 mM Tris-HCl buffer, pH 7.4).

Results and Discussion

Mass spectrometry

In order to study the reactivity of Cs_2IrCl_5CO with proteins, RNase A has been incubated in the presence of the Ir compound for 24 h in 1:10 protein to metal ratio and the resulting products have been analysed by electrospray ionization mass spectrometry (ESI-MS). Results of these analyses are reported in Figure 1. Spectra obtained in the presence of the Ir compound reveal that a number of different fragments can bind the protein. In particular, new peaks are detected in the ESI MS spectra, which have been assigned to a complex formed by RNase A with fragments of the type $-[IrCl_4CO]^-$ and $-[IrCl_3(H_2O)CO]$. Interestingly, more than one Ir fragment could bind the protein at the same time. The observation of these peaks suggests that the CO is retained upon protein binding, while a Cl^- ligand is released.

View Article Online
DOI: 10.1039/C6DT01685E

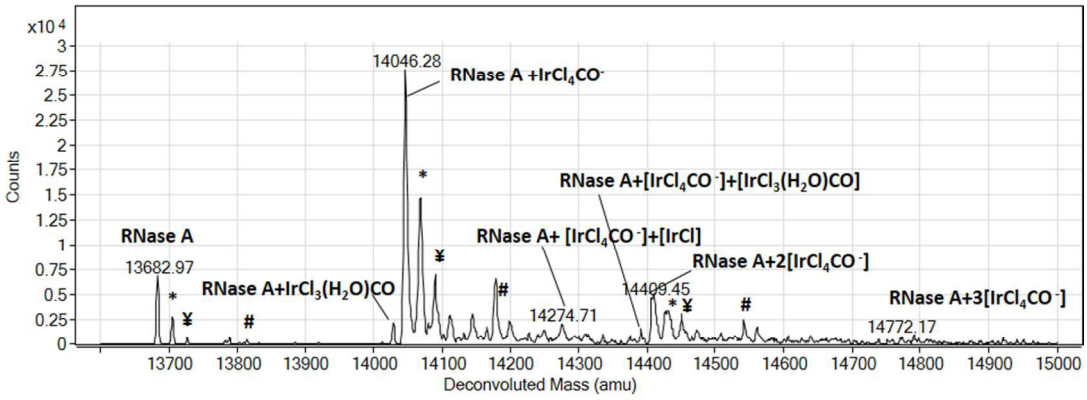

Figure 1. Deconvoluted ESI-MS spectra of RNase A incubated for 24 h at room temperature with 10^{-3} mol L^{-1} Cs_2IrCl_5CO dissolved in water (complex/protein=10:1) in 20 mmol L^{-1} ammonium acetate buffer, pH 6.8; symbols indicate several adducts of main peaks: *:RNase A+Na^+, ¥: RNase A+2Na^+, #: RNase A+Cs^+.

Circular dichroism studies

In order to verify the effect of the $IrCl_5CO^{2-}$ binding on RNase A structural stability, CD spectra have been recorded (Figure 2) and the signal intensity at 222 nm have been monitored for increasing temperature values (from 10 °C to 95 °C) (Figure 3). The far UV-CD spectra of RNase A and of the adduct formed upon 24 h of incubation of the protein in the presence of the Ir compound at a 1:1 and 1:10 protein to metal molar ratio are indistinguishable (Figure 2) at 10 °C in 10 mM Tris-HCl buffer, pH 7.4. They contain the typical fingerprints of α/β proteins. Furthermore, inspection of unfolding curves clearly indicates that the thermal denaturation of RNase A is not affected by the $IrCl_5CO^{2-}$ binding (Figure 3).

These findings demonstrate that binding of $IrCl_5CO^{2-}$ fragments to RNase A does not affect both protein overall conformation and structural stability.

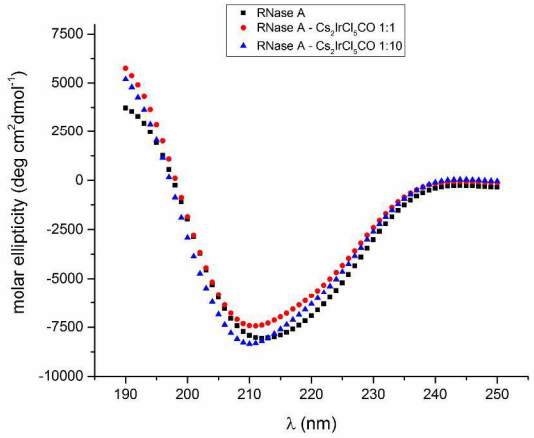

Figure 2. Far-UV CD spectra of RNase A and RNase A-$IrCl_5CO^{2-}$ adducts in 1:1 and 1:10 protein to metal molar ratio. Spectra have been acquired at 10 °C using a protein concentration of 0.1 mg mL^{-1} in a 10 mM Tris-HCl buffer, pH 7.4.

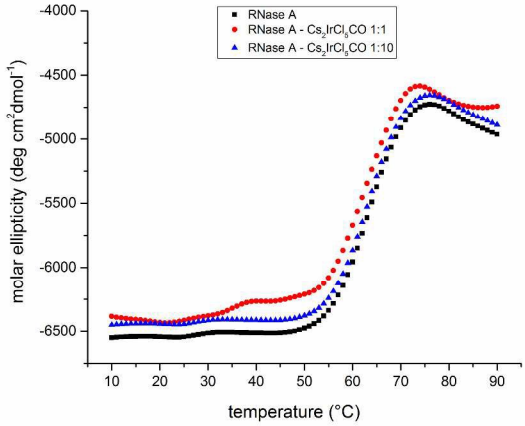

Figure 3. Thermal denaturation of RNase A and RNase A-$IrCl_5CO^{2-}$ adducts in 1:1 and 1:10 protein to metal molar ratio as followed by CD spectroscopy at 222 nm. Measurements were carried out in 10 mM Tris-HCl buffer, pH 7.4, using an enzyme concentration of 0.1 mg mL^{-1}. Heating rate was 1.0 °C min^{-1}.

Structure of the RNase A-$IrCl_5CO^{2-}$

To explore on a structural ground the reactivity of $IrCl_5CO^{2-}$ with RNase A, the structure of the adduct has been determined by X-ray crystallography, using two different datasets both collected using monoclinic crystals grown under the same conditions and containing two RNase A molecules in the asymmetric unit. These crystals differ in the time of soaking of the Ir compound. X-ray diffraction data on the first crystal were collected after four days of soaking in a saturated solution of Cs_2IrCl_5CO, whereas data on the second crystal after two months. Interestingly, the two structures show a different number of Ir-compound binding sites. Indeed, five sites have been identified in crystal 1 (N-terminal amine, Met29, His105 and His119 in molecule A and His119 in molecule B), whereas eight sites have been found in crystal 2 (N-terminal amine, Met29, His12, His105 and His119 in molecule A, His12, His105 and His119 in molecule B). In both cases, the structure of the protein is not significantly affected by the reaction with the CORM: the four disulphide bridges are retained

View Article Online
DOI: 10.1039/C6DT01685E

and the CA root mean square deviations from the ligand-free protein in the same experimental conditions (PDB code 1JVT) are in the range 0.19-0.42 Å.

Figure 4 illustrates the asymmetric unit content of the structures of the two RNase A-$IrCl_5CO^{2-}$ adducts.

The final model of the RNase A-$IrCl_5CO^{2-}$ adduct in crystal 1 (Figure 4A) includes 2238 non-hydrogen atoms and has been determined at 1.85 Å resolution. This structure refines to an R-factor of 0.172 (R-free 0.226). The average B-factor for all atoms of the structure is 26.4 $Å^2$. A full list of the refinement statistics is reported in Table 1. Figure 5 shows the 2Fo-Fc electron density map for the five Ir-compound binding sites identified in this structure. The occupancy factors for the Ir atoms are in the range 0.30-0.60. In molecule A, in the first Ir compound binding site, *i.e.* close to N-terminal amine, the Ir atom is bound to a Cl^- and is in contact with the side chain of Arg85 from a symmetry-related molecule (Figure 5A). This finding indicates that upon hydrolysis, Cs_2IrCl_5CO can act as a cross-linker bridging to different protein chains as already observed for cisplatin and other metallodrugs.[37-38] In this site, the electron density maps do not allow to complete the definition of the coordination sphere of Ir. In molecule A, at the binding site close to His105 side chain, the $[IrCl(H_2O)_3CO]^{2+}$ fragment is bound to the protein (Figure 5B). The same fragment is bound to the active site residue His119 of molecule B (Figure 5C). The product of the hydrolysis of this fragment, *i.e.* $[Ir(H_2O)_4CO]^{3+}$, is linked to Met29 side chain of molecule A (Figure 5D), with CO ligand that occupies an equatorial position with respect to Met side chain. The observation of this binding site is interesting. Indeed, although it is known that that Ir-based complexes can also bind to sulphur protein sites,[25] the interaction between sulphur containing residues and Ir complexes has never been described from a structural point of view. Finally, Ir compound fragment bound to His119 of molecule A presents a metal coordination shell completed by water molecules (Figure S1).

The structure of the RNase A-$IrCl_5CO^{2-}$ adduct in crystal 2 has been refined at a lower resolution (2.29 Å). This model includes 2027 non-hydrogen atoms and refines to an R-factor of 0.224 (R-free 0.293). In this structure, three additional Ir binding sites have been identified compared to those observed in crystal 1 (Figures 5E-F). The occupancy factors of the Ir atoms are in the range 0.30-1.00. A full list of the refinement statistics is reported in Table 1. The first two additional binding sites are close to His12 of the two molecules in the a.u., in the active site clefts. In these sites, the metal is bound to His12 and Gln11 side chains (Figure 5F) and is modelled as alternative to the Ir compound bound to His119. The other additional binding site is observed at the side chain of His105 of molecule B (Figure 5E). Here, a $[IrCl_2(H_2O)_2CO]^+$ fragment is bound to the protein. Interestingly, in this structure, the fragment bound to His119 of molecule B ($[Ir(H_2O)_4CO]^{3+}$) is different when compared to that found in crystal 1 ($[IrCl(H_2O)_3CO]^{3+}$, Figure 5C), suggesting that ligand exchange processes are possible upon protein binding.

Additional details on the Ir compound fragments identified in the two structures are reported in Table 2.

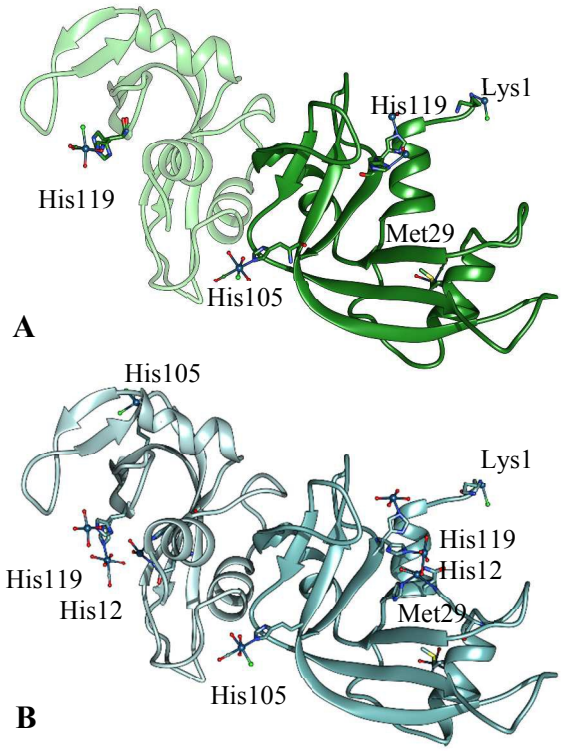

Figure 4. Cartoon diagram of the RNase A structures in the asymmetric unit from crystal 1 (A) and crystal 2 (B). Ir compounds are represented as ball and sticks, as well as the residues involved in the compound recognition (N-terminal Lys, His12, Met29, His105, and His119). Molecules A are on the right.

Raman microspectroscopic studies

Raman spectra have been collected to have an unambiguous evidence of the presence and persistency (no release) of CO inside the crystals of the adduct (Figure 6). As previously found,[25] the Cs_2IrCl_5CO powder shows signals due to Ir-Cl bond stretching in the 300-400 cm^{-1} region and a signal falling at about 2080 cm^{-1} assigned to the CO ligand.

The monitoring of the Raman spectra of RNase A crystals collected over 2 weeks of $IrCl_5CO^{2-}$ soaking shows that the metallodrug is able to enter within the protein crystals. The entrance into the crystal of the Ir compound is well evidenced by the appearance of a high-frequency band at 2073 cm^{-1} just after a few minutes of soaking. This spectral feature, due to the CO bound to the metal centre remains stable for two weeks, suggesting that under the investigated experimental conditions the CO ligand is not released by the compound. This observation is in contrast with the results obtained studying the reactivity of the same compound with HEWL in the crystal state.[19] In fact, it was previously shown that $IrCl_5CO^{2-}$ is able to release the CO ligand upon interaction with HEWL, with consequent appearance of new Raman spectral features in the 2000-2200 cm^{-1} region (CO stretching region, see Figures 9-10 in reference 25).

View Article Online
DOI: 10.1039/C6DT01685E

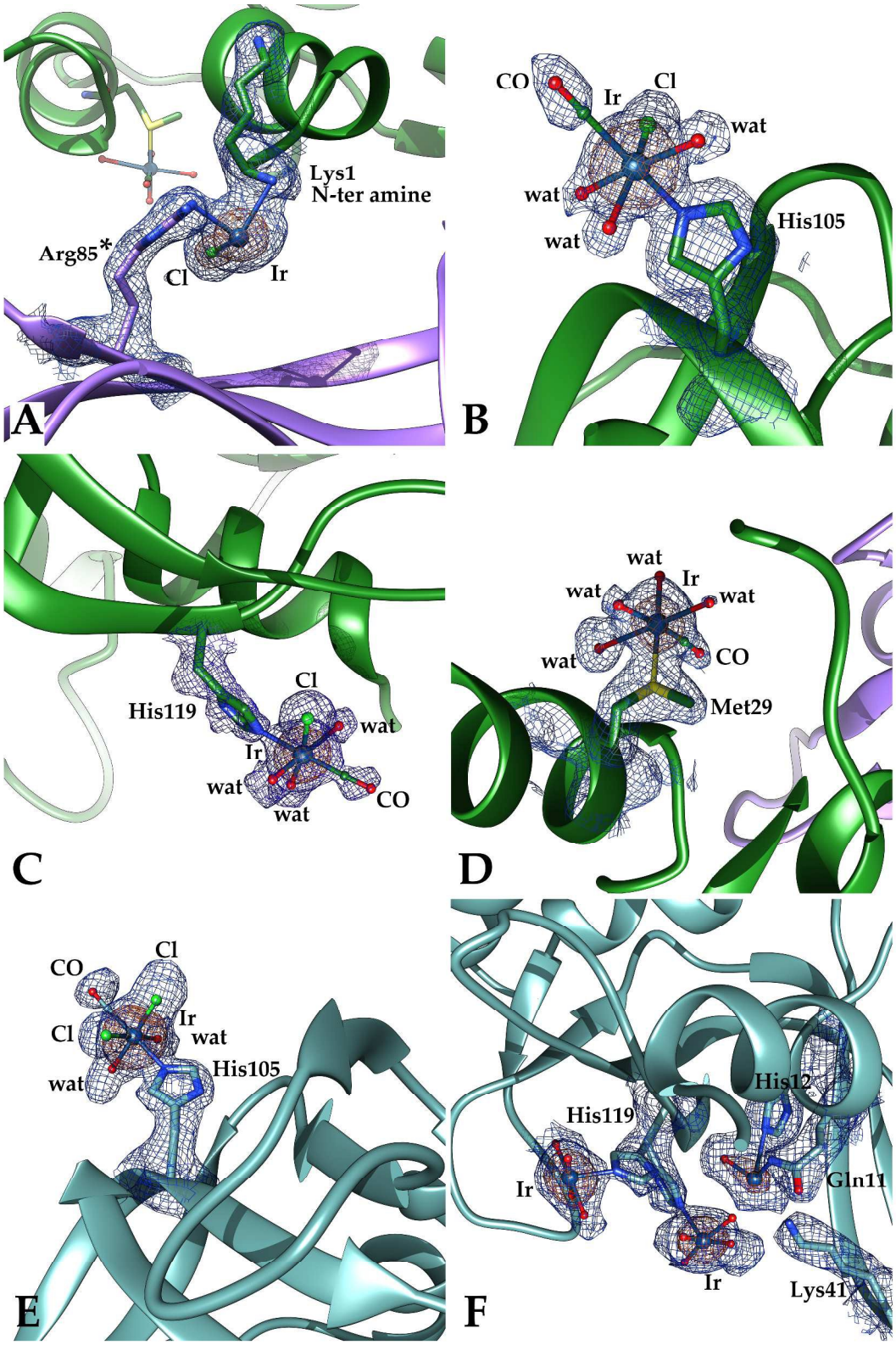

Figure 5. Details for the $IrCl_5CO^{2-}$ binding sites from crystal 1 (A-D) and for the additional $IrCl_5CO^{2-}$ binding sites from crystal 2 (E-F). (A) N-terminal amine (molecule A), (B) His105 (molecule A), (C) His119 (molecule B), (D) Met29 (molecule A); (E) His105 (molecule B of crystal 2); (F) His12 in the active site cleft (molecule A from crystal 2). 2Fo-Fc electron density map is contoured at 1.5 σ (blue) and 2.5 (orange) level.

View Article Online
DOI: 10.1039/C6DT01685E

Table 2. Additional details on the Ir compound fragments identified in the two structures of RNase A- $IrCl_5CO^{2-}$ and on the interactions that they form with protein residues

	Crystal 1				Crystal 2			
Chain	**Site**	**Fragment***	**Interaction**	**Distance (Å)**	**Site**	**Fragment***	**Interaction**	**Distance (Å)**
A	**His 105**	$[IrCl(H_2O)_3CO]^{2+}$	Ir E – Cl 2	2.0	**His 105**	$[IrCl(H_2O)_3CO]^{2+}$	Ir E – Cl 3	2.3
			Ir E – HOH 3	2.0			Ir E – HOH 2	2.0
			Ir E – HOH 4	2.3			Ir E – HOH 4	2.0
			Ir E – HOH 5	2.5			Ir E – HOH 5	2.0
			Ir E – NE2	2.2			Ir E – NE2	2.3
			Ir E – C 6	2.3			Ir E – C 6	2.0
	Met 29	$[Ir(H_2O)_4CO]^{3+}$	Ir L – C 2	2.0	**Met 29**	$[IrX(H_2O)_3CO]^{3+}$	Ir L – C 2	2.0
			Ir L – HOH 3	2.6			Ir L – HOH 3	2.0
			Ir L – HOH 4	2.9			Ir L – HOH 4	2.0
			Ir L – HOH 5	2.6			Ir L – HOH 5	2.0
			Ir L – HOH 6	2.0			Ir L – SD 29	2.3
			Ir L – SD	2.6				
	His 119 A	$[Ir(H_2O)_2X_3]^{3+}$	Ir G/A – HOH 2/A	2.0	**His 119 A**	$[Ir(H_2O)_4X]^{3+}$	Ir G/A – His119/A NE2	2.2
			Ir G/A – HOH 260	2.7			Ir G/A – HOH 2/A	2.0
			Ir G/A – His 119 ND1/A	2.6			Ir G/A – HOH 3/A	2.0
			Ir G/A – His 119 ND1/B	2.4			Ir G/A – HOH 4/A	2.0
							Ir G/A – HOH 5/A	2.0
	His 119 B	$[Ir(H_2O)_3X_2]^{3+}$	Ir G/B – His119 NE2/B	2.3	**His 119 B**	$[Ir(H_2O)_4X]^{3+}$	Ir G/B – His119/B NE2	2.3
			Ir G/B – HOH 2/B	2.4			Ir G/B – HOH 2/B	2.0
			Ir G/B – Glu111 OE2/B	3.0			Ir G/B – HOH 3/B	2.0
			Ir G/B – HOH 134	2.9			Ir G/B – HOH 4/B	2.0
			Ir G/B – HOH 199*	2.8			Ir G/B – HOH 5/B	2.0
	Lys 1	$[IrClX_4]^{2+}$	Ir F – Lys1 N	2.8	**Lys 1**	$[IrClX_4]^{2+}$	Ir M – Cl 2	2.6
			Ir F – Cl 2	2.3			Ir M – N	2.3
			Ir F – Arg85* NH2	2.7				
					His 12	$[Ir(H_2O)X_4]^{3+}$	Ir J/A – His12 NE2	2.8
							Ir J/A – HOH 2/A	2.0
							Ir J/A – Gln11 NE2	2.6
B	**His 119 A**	$[IrCl(H_2O)_3CO]^{2+}$	Ir I/A – Cl 2/A	2.7	**His 119 A**	$[Ir(H_2O)_4CO]^{3+}$	Ir I/A – His 119/A NE2	2.2
			Ir I/A – HOH 3/A	2.5			Ir I/A – HOH 2/A	2.0
			Ir I/A – HOH 4/A	2.0			Ir I/A – HOH 3/A	2.0
			Ir I/A – HOH 5/A	2.0			Ir I/A – HOH 4/A	2.0
			Ir I/A – C 6/A	2.0			Ir I/A – HOH 5/A	2.0
			Ir I/A – His119/A NE2	2.2			Ir I/A – C 6/A	2.0
					His 119 B	$[Ir(H_2O)_4X]^{3+}$	Ir I/B – His 119/B NE2	1.9
							Ir I/B – HOH 2/B	2.0
							Ir I/B – HOH 3/B	2.0
							Ir I/B – HOH 4/B	2.0
							Ir I/B – HOH 5/B	2.0
					His 105	$[IrCl_2(H_2O)_2CO]^{+}$	Ir F – Cl 2	2.2
							Ir F – Cl 3	2.6
							Ir F – HOH 4	2.0
							Ir F – HOH 5	2.6
							Ir F – NE2	2.2
							Ir F – C	2.0
					His 12	$[Ir(H_2O)X_4]^{3+}$	Ir K/B – His12 NE2	2.7
							Ir K/B – HOH 2/B	2.1
							Ir K/B – Gln11 NE2	2.6

*water molecule ligands in the identified Ir compound fragments could be deprotonated.

View Article Online
DOI: 10.1039/C6DT01685E

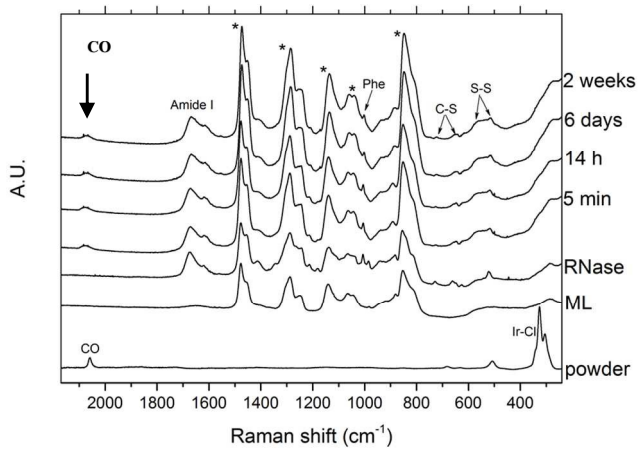

Figure 6. Raman spectra of Cs_2IrCl_5CO powder, RNase A crystal and of protein crystals soaked in a saturated solution of Cs_2IrCl_5CO as a function of time. Star refers to signals from the buffer. Excitation line 514 nm; power at the sample 3 mW; spectral resolution 7 cm^{-1}. CO band persistency indicates that no CO release is occurring in the crystals of the adduct.

Interestingly, when compared to previous studies, other differences also appear. In fact, differently from previous Raman data collected on lysozyme-$IrCl_5CO^{2-}$ adduct (collected using crystals grown in 1.2 M NaCl)[25], in the present case, the major Raman band around 300 cm^{-1}, related to Ir-Cl stretching, seems attenuated. This indicates that under the NaCl-free conditions used to study the formation of the RNase A-$IrCl_5CO^{2-}$ adduct, the Ir compound probably undergoes to the hydrolysis reaction. The slower Cl^-/H_2O exchange observed for the HEWL-$IrCl_5CO^{2-}$ adduct when compared to RNase A-$IrCl_5CO^{2-}$ is probably related to the high concentration of Cl^- ions in the solution used to grow HEWL crystals.

Conclusions

The interaction between CO-releasing compounds and biological macromolecules has received increasing attention over the past decade. Here we have reported a combined spectrometric/spectroscopic/crystallographic study to unveil the molecular bases of the protein/Ir-based CORM recognition.

The results reported in this work allow to draw the following conclusions:

a) $IrCl_5CO^{2-}$ tightly binds RNase A at N-terminal amine and at His12, His105, His119 and Met29 side chains. His residues have been found to bind Ir-based metallodrugs in other structures[25], but details of Met-Ir interactions and binding to N-terminus were never shown before. Sulfur-containing ligands are often strong binding sites for the heavy transition metal ions. For example, it has been shown that cisplatin and carboplatin bind to the sulfur of Met29 of RNase A,[6,39-41] to sulphur of Met65 of cytochrome c[42] and to Met side chains of Na+/K+ ATPase[43] and human serum albumin[44].

b) $IrCl_4CO^{2-}$ and the products of its hydrolysis bind the protein

c) the formation of the adduct does not affect significantly the overall enzyme structure

d) the RNase A-$IrCl_5CO^{2-}$ adduct is stable under the investigated experimental conditions

e) the adduct formed in the reaction between RNase A and the $IrCl_5CO^{2-}$ compound retains a significant amount of CO for at least two months, further confirming the idea that the formation of complexes between protein and CORM can be used to modulate the kinetics of the CO release[25,45-46].

f) The adduct has the same thermal stability of the ligand-free protein.

It is interesting to discuss this work in the general framework of iridium compound-protein interaction.

Iridium complexes have received considerable attention in catalysis,[47] optoelectronics and inorganic photochemistry[47-48], medicinal inorganic chemistry and biology[49]. Furthermore, they can be used as chemosensors, for live cell imaging, in vivo tumor imaging[50] and as protein-protein interaction inhibitors. It has been shown that negatively charged Ir complexes like $(IrCl_6)^{3-}$ can bind basic protein regions. Ir complexes can bind His residues by nucleophilic substitution of a metal ligand, usually a chloride, by the imidazole.[25] Taking advantages of these properties, the cyclometalated Ir(III) solvato complex $[Ir(ppy)_2(solv)_2]^+$ has been used as a selective luminescent switch-on probe for His-rich proteins.[51] In contrast, positively charged complexes like $(Ir(NH_3)_6)^{3+}$ may bind to acidic regions on the protein (http://homepage.usask.ca/~pag266/bart-hazes.html).

Here, we have shown that Ir(III) complexes are also able to bind to Met side chains and N-terminal amines. This finding could help in the understanding or predicting biomolecules-Ir compounds interactions. Our data can be used to perform statistical analysis on the features of preferred Ir binding sites on protein surfaces that could be of help for future drug-design.

As a final comment, it could be noted that the two Raman studies on lysozyme and RNase A with $IrCl_5CO^{2-}$ suggest a possible correlation between CO-releasing ability of the Ir compound and its Cl^-/H_2O content, at least in the time scale of the Raman analysis (2 weeks): the higher is the content of Cl^- in the coordination sphere, the faster is the CO release within the crystal, but further studies are needed to verify this hypothesis.

Acknowledgement

The authors thank Giosuè Sorrentino and Maurizio Amendola for technical assistance.

Notes and references

*‡ *Department of Chemical Sciences, University of Naples Federico II, Complesso Universitario di Monte Sant'Angelo, Via Cintia, I-80126, Napoli, Italy. Fax: +39081674090; Tel: +39081674276; E-mail: antonello.merlino@unina.it*

† *Departamento de Química Inorgánica, Analítica y Química Física/INQUIMAE-CONICET, University of Buenos Aires, Ciudad Universitaria, Pab. 2, C1428EHA Buenos Aires, Argentina*

CNR Institute of Biostructures and Bioimages, Via Mezzocannone 16, Napoli, Italy.

¥ *Department of Pharmacy, University of Naples Federico II,*

View Article Online
DOI: 10.1039/C6DT01685E

(1) W. H. Ang, A. Casini, G. Sava, P. J. Dyson, *J. Organomet. Chem*. 2011, 696, 989–998.
(2) (a) A. Casini, A. Guerri, C. Gabbiani, L. Messori, *J. Inorg. Biochem*. 2008, 102, 995–1006; (b)A. Casini, C. Gabbiani, G. Mastrobuoni, L. Messori, G. Moneti,G.Pieraccini. *ChemMedChem* 2006, 1, 413–417.
(3) E. Meggers, *Chem. Commun*. 2009, 1001–1010;
(4) (a) A. Casini, J. Reedijk. *Chemical Science* 2012, 3, 11, 3135–3144; (b) A.R. Timerbaev, C.G. Hartinger, S.S. Aleksenko, B.K. Keppler Chem. Rev. 2006, 106, 2224-2248.
(5) S. M. Mejer, M. V. Babak, B. K. Keppler, C. H. Hartinger. *ChemMedChem* 2014, 9, 1351–1355; A. R. Timerbaev, K. Pawlak, C. Gabbiani, L. Messori. Trends in Analytical Chemistry 2011, 30, 7, 1120–1138
(6) L. Messori, A. Merlino, *Coord Chem Rev*. 2016, 315, 67.
(7) (a) G. C. Hartinger, P .J. Dyson, Chem Soc Rev 2009, 38, 391; (b) C. C. Romao, W. A. Blatter, J. D. Seixas, G. J. Bernardes, Chem Soc. Rev 2012, 41, 3571.
(8) (a) R. Motterlini, P. Sawle, J. Hammad, S. Bains, R. Alberto, R. Foresti, C. J. Green, *Faseb J.* 2005, 19, 284; (b) T. R. Johnson,. B. E. Mann, J. E. Clark, R. Foresti, C. J. Green, R. Motterlini, *Angew. Chem. Int. Ed.* 2003, 42, 3722.
(9) R. Motterlini, J. E. Clark, R. Foresti, P. Sarathchandra, B. E. Mann, C. J. Green, *Circ Res* 2002, 90, E17.
(10) M. D. Pizarro, J. V. Rodriguez, M. E. Mamprin, B. J. Fuller, B. E. Mann, R. Motterlini, E. E. Guibert, *Cryo-biology* 2009, 58, 248.
(11) M. Desmard, K. S. Davidge, O. Bouvet, D. Morin, D. Roux, R. Foresti, J. D. Ricard, E. Denamur, R. K. Poole, P. Montravers, R. Motterlini, J. Boczkowski, *Faseb J.* 2009, 23, 1023.
(12) J. Atkin, S. Williams, P. Sawle, R. Motterlini, J. M. Lynam, I. J. Fairlamb, *Dalton Trans* 2009, 19, 3653.
(13) P. V. Simpson, , K. Radacki, H. Braunschweig, U. Schatzschneider. J *Organ Chem* 2015, 782, 116.
(14) D. E. Bikiel, E. Gonzalez Solveyra, F. Di Salvo, H.M. Milagre, M. N. Eberlin, R. S. Correa, J. Ellena, D. A. Estrin, F. Doctorovic, *Inorg. Chem* 2011, 50, 2334.
(15) M. G. Bani-Hani, D. Greenstein, B. E. Mann, C. J. Green, R. Motterlini, *Pharmacol. Rep*. 2006, 58 Suppl, 132.
(16) R. Motterlini, B.Haas, R. Foresti, *Med. Gas Res*. 2012, 2, 28.
(17)N. Schallner, S. Schwemmers, C. I. Schwer, C. Froehlich, P. Stoll, M. Humar, H. L. Pahl, A. Hoetzel, T. Loop, U. Goebel, *Eur. J. Pharmacol*. 2011, 670, 58.
(18) J. L. Wilson, H. E. Jesse, B. M. Hughes, V. Lund, K. Naylor, K. S.Davidge, G. M. Cook, B. E. Mann, R. K. Poole, *Antioxid. Redox Signa*l 2013, 19, 497.
(19) C. I. Schwer, M. Mutschler, P. Stoll, U. Goebel, M. Humar, A. Hoetzel, R. Schmidt, *Mol. Pharmacol* 2010, 77, 660.
(20) R. S. Herrick, C. J. Ziegler, T. C. Leeper, *J. Organomet. Chem.* 2014, 751, 90.
(21) T. Santos-Silva, A. Mukhopadhyay, J. D. Seixas, G. J. Bernardes, C. C. Romao, M. J. Romao, *J. Am. Chem. Soc*. 2011, 133, 1192.
(22) T. Santos-Silva, A. Mukhopadhyay, J. D. Seixas, G. J. Bernardes, C. C. Romao, M. J. Romao, *Curr. Med. Chem*. 2011, 18, 3361.
(23) M. F. A.; Santos, J. D. Seixas, A. Coelho, A. Mukhopadhyay, P. M. Reis, M. J. Romao, C. C. Romao, T. J. Santos-Silva, *Inorg. Biochem.* 2012, 117, 285.
(24) J. D. Seixas, A. Mukhopadhyay, T. Santos-Silva, L. E. Otterbein, D. J. Gallo, S. S. Rodrigues, B. H. Guerreiro, A. M. L. Goncalves, N. Penacho, A. R. Marques, A. C. Coelho, P. M. Reis, M. J. Romao, C. C. Romao, *Dalton. Trans*. 2013, 42, 5985.
(25) A. A. Petruk, A. Vergara,; Marasco, D. Bikiel, F. Doctorovich, D.A. Estrin, A. Merlino, *Inorg Chem*. 2014, 53, 10456.
(26) I. Russo Krauss, F. Sica, C.A. Mattia, A. Merlino, *Int. J. Mol. Sci*. 2012, 13, 3782.
(27) I. Russo Krauss, L. Messori, M.A. Cinellu, D. Marasco, R. Sirignano, A. Merlino, *Dalton Trans*. 2014, 43, 17483.
(28) L. Messori, M. A. Cinellu, A. Merlino, *ACS Med Chem Lett*. 2014, 5, 1110.
(29) L. Messori, F. Scaletti, L. Massai, M.A. Cinellu, C. Gabbiani, A. Vergara, A. Merlino, *Chem Commun (Camb*). 2013, 49, 10100.
(30) W. Minor, M. Cymborowski, Z. Otwinowski, M. Chruszcz, *Acta Cryst. D* 2006, 62, 859.
(31) L. Vitagliano, A. Merlino, A. Zagari, L. Mazzarella, *Proteins*. 2002, 46, 97.
(32) L. Vitagliano, A. Merlino, A. Zagari, L. Mazzarella, *Protein Science* 2000, 9, 1217.
(33) G. N. Murshudov, P. Skubak, A. A. Lebedev, N. S. Pannu, R.A. Steiner, R. A. Nicholls, M. D. Winn, F. Long, A. A. Vagin, *Acta Crystallogr., Sect. D: Biol. Crystallogr.,* 2011, 67, 355.
(34) P. Emsley, B. Lohkamp, W. G. Scott, K.Cowtan, *Acta Crystallogr D Biol Crystallogr*. 2010, 66, 486.
(35) E.F. Pettersen, T.D. Goddard, C.C. Huang, G.S. Couch, D.M. Greenblatt, E.C. Meng, T.E. Ferrin, *J Comput Chem*. 2004, 25, 1605.
(36) A. Vergara, A. Merlino, E. Pizzo, G. D'Alessio, L. Mazzarella, *Acta Cryst.* D 2008, 64, 167.
(37) D. Picone, F. Donnarumma, G. Ferraro, I. Russo Krauss, A. Fagagnini, G. Gotte, A. Merlino, *J. Inorg Biochem.* 2015, 146, 37.
(38) W.H. Ang, L.J. Parker, A. De Luca, L. Juillerat-Jeanneret, C. J. Morton, M. Lo Bello, M.W. Parker, P.J. Dyson, *Angewandte Chemie-International Edition,* 2009, 48, 3854.
(39) L. Messori, A. Merlino, *Inorg Chem*. 2014, 53, 3929.
(40) D. Picone, F. Donnarumma, G. Ferraro, I. Russo Krauss, A. Fagagnini, G. Gotte, A.Merlino, *J Inorg Biochem*. 2015, 146, 37.
(41) L. Messori, T. Marzo, A. Merlino, *J Inorg Biochem.* 2015, 153, 136.
(42) G. Ferraro, L. Messori, A. Merlino, *Chem Commun (Camb).* 2015, 51, 2559.
(43) M. Huliciak, L. Reinhard, M. Laursen, N. Fedosova, P. Nissen, M. Kubala, *Biochem Pharmacol*. 2014, 92, 494.
(44) G. Ferraro, L. Massai, L. Messori, A. Merlino, *Chem Commun (Camb).* 2015, 51, 9436.
(45) H. Tabe, K. Fujita, S. Abe, M. Tsujimoto, T. Kuchimaru, S. Kizaka-Kondoh, M. Takano, S. kitagawa, T. Ueno, *Inorg Chem* 2015, 54, 215.
(46) M. Chaves-Ferreira, I. S. Albuquerque, D. Matak-Vinkovic, A. C. Coelho, S. M. Carvalho, L. M. Saraiva, C. C. Romao, and G. J. L. Bernardes, *Angew. Chem. Int. Ed*. 2015, 54, 1172.
(47) R. Crabtree. *Acc. Chem. Res.*, 1979, 12 (9), 331–337
(48) Z. T. Yu. Organometallics and Related Molecules for Energy Conversion. Part of the series Green Chemistry and Sustainable Technology pp 513-537
(49) C. E. Housecroft. Iridium: Inorganic & Coordination Chemistry. Encyclopedia of Inorganic Chemistry. 2006. J., Wiley and Sons. DOI: 10.1002/0470862106.ia101
(50) S. Zhang, M. Hosaka, T. Yoshihara, K. Negishi, Y. Iida, S. Tobita, T. Takeuchi. *Cancer Res*. 2010, 70(11), 4490-8.
(51) K. M. Davis, A. L. Bitting, C. F. Markwalter, W. S. Bauer, D. W Wright, *Journal of Visualized Experiments* 2015, 101, e52856.